Research in Astron. Astrophys. **2009** Vol. **9** No. **9**, 1011–1023
http://www.raa-journal.org *http://www.iop.org/journals/raa*

***R**esearch in*
***A**stronomy and*
***A**strophysics*

Scale errors in the photometry of some CCD standard fields

Bao-An Yao[1] and R. D. Cannon[2]

[1] Shanghai Astronomical Observatory, Chinese Academy of Sciences, Shanghai 20030, China; *yba@shao.ac.cn*
[2] Anglo-Australian Observatory, Epping, NSW2121, Australia

Received 2008 November 25; accepted 2009 June 28

Abstract There is a scale error, i.e., a systematic dm which is a function of magnitude, in the CCD photometry of NGC 7790, NGC 4147 and NGC 7006 published by Odewahn et al. The scale error also exists in the CCD photometry of NGC 7790 by Petrov et al. The reason why this kind of error, which may only exist in photographic photometry, appears in a linear detector such as a CCD, is not immediately clear. If the CCD systems used by Odewahn et al. and Petrov et al. are really linear, maybe it is related to their use of the variable aperture technique in the former and the reduction method in the latter.

Key words: techniques: photometric — CCD

1 INTRODUCTION

In order to provide calibration for CCD photometry, several fields in the vicinity of star clusters were observed as standard fields by Christian et al. (1985, hereafter C85). This was the first attempt to bridge the gap between detailed photoelectric measurements and two-dimensional imagery. They hoped that the photometric precision of the published standard values would be improved through repeated observations of these fields with CCDs and later extended to fainter magnitudes. After repeated CCD observations, Odewahn et al. (1992, hereafter Od92) improved the accuracy of the standards and extended them to fainter magnitudes using aperture photometry. Only uncrowded stars were selected by them. In the process of using these fields, some standard stars which appear to be crowded with faint neighbors in NGC 7790 were already pointed out by Yao (1998) (in that paper, the scale error was not recognized). However, the scale errors existing in the CCD photometry of Od92 are beyond expectation. NGC 7790 was the first to be found, NGC 4147 was the second, and the third cluster NGC 7006 was last. Thus, all the standard CCD fields observed by Od92 were not suitable to be used as standards without correction, though the given precision is high for many stars in their list. We submitted an unpublished research note pointing out the existence of the scale error in 1998. In 2000, Stetson (2000, hereafter St00) published the largest sample of precise BVRI standards. Od92's photometry was not combined into his sample because Stetson realized the existence of the systematic error. Petrov et al. (2001, hereafter Pe01) have extended Od92's BVR sequences into U and I. They still take Od92's sequences as the standards and their published BVR magnitudes also suffer from the scale error. In addition, the scale error also exists in their I photometry. The evidence is given as follows.

2 SCALE ERRORS IN THE PHOTOMETRY OF NGC 7790

Our original purpose for observing NGC 7790 was to calibrate the old open cluster NGC 188 (Cannon & Yao, in preparation). The data were obtained with the 2.5-m Isaac Newton telescope (INT) on La

Palma in 1987 using the prime focus RCA 320×512 CCD (pixel size 30 by 30 microns) by Griffiths and Buttress. An image scale of 0.74 arcsec per pixel (worse than 0.654 in Od92) results in a field of 4.0 by 6.3 arcmin. The readout noise is about 60e$^-$ and the gain is 4e$^-$ adu^{-1}. The linear range for this RCA CCD is only 35 000 adu, though the saturation is $> 60\,000$ adu (Unger et al. 1988). We never measure stars with pixel values higher than 34 000 adu in the reduction. The exposure time was 50 s for B and 40 s for V. The recorded seeing was about $2''$ but the real measured FWHM was from 2 to 2.6 pixels, so the images were somewhat undersampled. All the defects in undersampling appeared in our photometry (the star image is easily saturated; the counts of a star depend on the position where the star falls, at the center of a pixel or at the node of the pixels; there is no perfect psf fitting, etc.). The instrumental magnitudes were obtained by running ALLSTAR of DAOPHOT (Stetson 1987) in IRAF in the normal ways. The shape of the psf is varied across the whole CCD frame. All six options of the psf function in DAOPHOT were tried and the best one was selected to be reduced (in this case Penny1 or Moffat25). In order to fit the whole frame, a variable psf must be used. Though VA=2 (psf varies quadratically with position) was used in the fit, the residuals on the subtracted CCD frame still show some systematic difference.

Concerning the character of the RCA CCD, IRAF users might have read the note written by Massey & Davis (1992) that the advertised linear dynamic range is 32767 adu (72 ke$^-$ after bias is allowed for), but their practice showed that only stars with peaks of 18 kadu (a mere 40 ke$^-$) were safe to use in the psf analysis, so the dynamic range was simply not quite as advertised. Although the psf function broke down above 18 K, the chip remained "linear" in the sense that aperture photometry continued to give good results - the total number of counts continued to scale right up to the A/D limit of 32767 adu. "This appears to be a subtle charge transfer problem." This effect was not found for the RCA CCD at INT, and we cannot scale right up to 60 000 adu in aperture photometry, but we suffer from another effect. If a normal fitting radius (nearly equal to the FWHM) is used in the psf analysis or a normal software aperture (the radius of the aperture is about 0.8 to 1.5 FWHM) is used in aperture photometry for the stars in the open cluster NGC 188 (declination 85°), both of the results will show scale errors for the faint stars, which is not due to an obvious cause (Cannon and Yao, in preparation). The scale error can be decreased by increasing the radius of the software aperture and it almost disappears when the radius becomes large enough at the price of losing precision for faint stars. The larger the radius, the larger the random error for the fainter stars and the shorter the magnitude range while having reasonable precision. Besides, more and more stars cannot be measured as isolated stars in this way. This effect is less obvious for NGC 7790 (declination 61°) but it still exists. As shown below, the value of the coefficient to describe the scale error in our psf analysis photometry is less than 0.01. In order to measure as many stars as possible in NGC 7790 to compare with others, we present here the psf analysis results with a fitting radius of 3. In summary, the precision returned from ALLSTAR was not high, about 0.02 mag even for the brightest measurable stars in our photometry for one CCD frame. We used five exposures for B and five for V in NGC 7790, and the averaged values with higher precision are used to compare with the photometry of Od92.

Figures 1 and 2 show the comparisons of the common stars between our instrumental magnitudes and those of Od92, where the lower-case letters refer to the former and the upper-case to the latter. While the scatter of the stars for a given magnitude along the x axis direction reflects the color equation between the two systems plus random error, the stars for a given color should be distributed vertically along the y axis direction if no scale error exists in the photometry. Contrary to expectation, the scale errors do appear both in B and V. Needless to say, there is a mixture of color equations with scale error and random error. If the equations $dV = v - V = a + b \times V + c \times (B - V)$ and $dB = b - B = a' + b' \times B + c' \times (B - V)$ are used to fit the relations in Figures 1 and 2, then we get $a = 0.29 \pm 0.08$, $b = -0.036 \pm 0.005$, $c = 0.01 \pm 0.02$, $a' = 0.40 \pm 0.05$, $b' = -0.031 \pm 0.003$, and $c' = -0.08 \pm 0.01$. However, we have encountered a strange effect in the psf photometry (a normal fitting radius resulted in a scale error). In the following, we show that the above scale errors mainly originate from Od92. First, our v values have been compared with the measurements taken with the 1.56-m reflector at the Shanghai Observatory on 1997 November 5 using a Thomson 1024×1024 CCD camera through the V filter (image scale $0.26''$/pixel). The linear range of this CCD camera is right up to 60 000 adu. The exposure was 100 s. The reduction was the same as above. As shown in Figure 3, there is negligible scale error, if any, though the color equation is obvious and the random scatter is not small due to the low input signal to noise ratio (the transparency was not good on 1997 November 5). Using the equation $v' - v = a_1 + b_1 \times v + c_1 \times (b - v)$ to fit the relation in Figure 3, the value of a_1 is 0.15±0.08, b_1 is -0.002 ± 0.005 and $c_1 = -0.17 \pm 0.02$. Here, v' refers to the instrumental magnitudes of the 1.56-m reflector while b and v to that of INT. When the v is transformed to v' using the above equation (but letting $b_1 \times v = -0.002 \times 15.0 = \mathrm{const}$, and considering that there is no scale error because the value of b_1 itself is less than the error), the residuals vs. v values are shown in Figure 4. However, the scale error appears in Figure 5 where the $v's$ are compared with the Vs of Od92. Using equation $v' - V = a'_1 + b'_1 \times V + c'_1 \times (B - V)$ to fit the relation, then $a'_1 = 0.65 \pm 0.10$, $b'_1 = -0.035 \pm 0.007$, and $c'_1 = -0.13 \pm 0.02$. Comparing the value of 0.002 with the value of 0.035, the conclusion that the main photometry of Od92, which suffers from the scale error, is safe.

To definitely confirm the scale error in Od92, a comparison between Od92 and C85 should be straightforward because the observations of Od92 were tied to the C85 photometry. However, the number of stars in C85 is small and the accuracy is low. There is a note on the photometry of NGC 7790 in C85 pointing out that the "RMS variations of NGC 7790 data worse than expected, cause is not immediately obvious." We note that one of the causes may be that the uncrowded stars selected by C85 are in fact crowded stars. Specifically, the star 16 (= Od58) has three neighbors with differential magnitudes 2.1, 4.5 and 5.1 (all in V) and differential distances 2.2, 2.8 and 6.6 (in arcsec) respectively. Relative to the main star, star 17 (= Od59) has one neighbor with differential magnitude 4.0 and differential distance 2.0. Star 21 (= Od77) has a less influential neighbor with differential magnitude 5.2 and differential distance 4.3. Star 9's (= Od62) neighbor may be neglected (with a differential magnitude of 5.6 and differential distance of 4.8) (Yao 1998). Star 25's image has appeared as a crowded star in figure 5 of Od92 already so Od92 did not take it as a standard star. In fact, 25's neighbor has a differential magnitude of 2.1 in V and a differential distance of 4 arcsec, so a certain percentage of the light of the star was included in the 10-arcsec diaphragm of the photoelectric photometer in C85. The percentage varies with imperfect centering. If we delete stars 16, 17, 21, and 25 and only compare the other six stars, the scale error clearly stands out in Figure 6 with rather small scatter except for star 100 (=Od51). We have not checked star 100 so we have no explanation of this star for the time being. Here $a''_1 = 0.23 \pm 0.05$, $b''_1 = -0.016 \pm 0.003$, and $c''_1 = 0.005 \pm 0.008$ (Od51 is deleted in the calculation).

In 1999, the unpublished CCD photometry of Davis (1999) was kindly given to us by her. Comparison between Od92 and that of Davis (hereafter Da99) is given in Figure 7 (for V). There are 19 stars in NGC 7790 in Da99 but only 18 common stars can be compared. We deleted star Od58 in the calculation and obtained the scale error $b_2 = -0.027 \pm 0.005$. A similar comparison between Od92 and Da99 for B is shown in Figure 8, where the scale error is $b_3 = -0.017 \pm 0.004$.

When our INT data is compared with Da99, a small scale error appears in Figure 9. We have 14 common stars with Da99 but only 12 stars are used in comparison (delete Od98 and 104 due to too large deviations). Here, the scale error is $b_4 = 0.003 \pm 0.003$. We suppose that this small scale error mainly originates from our photometry. However, comparing the value 0.003 with 0.027, the scale error in Od92 is definite.

Inspecting all of the above figures carefully, one can see that the scale error in Od92 is changing from bright to faint stars. The fainter the star image, the larger the scale error. The straight lines in the figures only represent the average relationship.

Da99 is also compared with C85. All the 9 common stars between them are plotted in Figure 10 (for V) but only six stars (Od51, 58, 72, 77, 88, 97) are used to calculate the equation because Od59 is a double star (see above) and stars Od62, 65 have large deviations (cause unknown). Here, the crowded star Od58 has no large deviation, and to include it or not in the calculation has negligible influence. We get $a_5 = 0.08 \pm 0.06$, $b_5 = -0.006 \pm 0.004$, and $c_5 = -0.001 \pm 0.001$. Though the comparison here uses small number statistics, it seems that the small scale error is real. A similar comparison for B is shown in Figure 11. Here, the scatter is not small, and all the 9 common stars together in Figure 11 do not show reliable estimations of the scale error. We get $b_6 = -0.001 \pm 0.008$. We also compared our INT data with C85. Unfortunately, there are only 5 uncrowded common stars to do small number

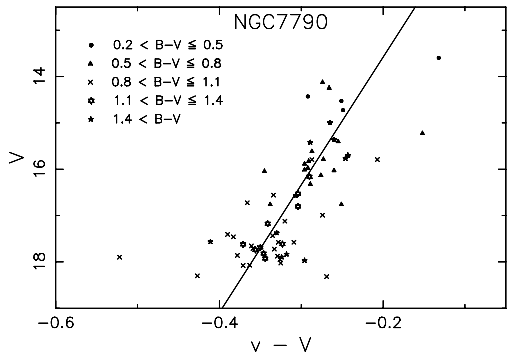

Fig. 1 Relationship between $v - V$ and V. The straight line represents the equation $v - V = a + b \times V + c \times (B - V)$ for $(B - V) = 0.65$. Here $b = -0.036$ while it should be zero if no scale error exists.

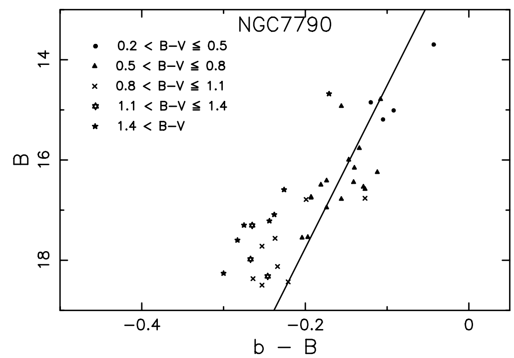

Fig. 2 Relationship between $b - B$ and B. The straight line represents the equation $b - B = a' + b' \times B + c' \times (B - V)$ for $(B - V) = 0.65$. Here $b' = -0.031$.

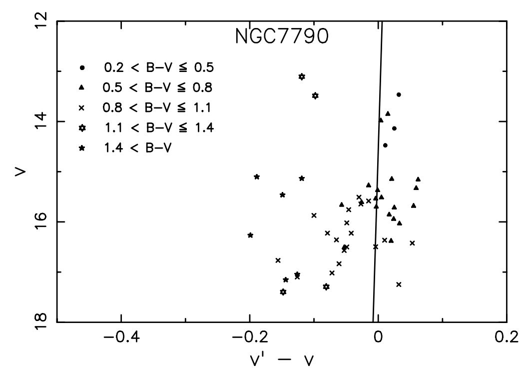

Fig. 3 Relationship between $v' - v$ and v. The straight line represents the equation $v' - v = a_1 + b_1 \times v + c_1 \times (b - v)$ for $(b - v) = 0.7$. Here $b_1 = 0.002$ shows negligible scale error, if any.

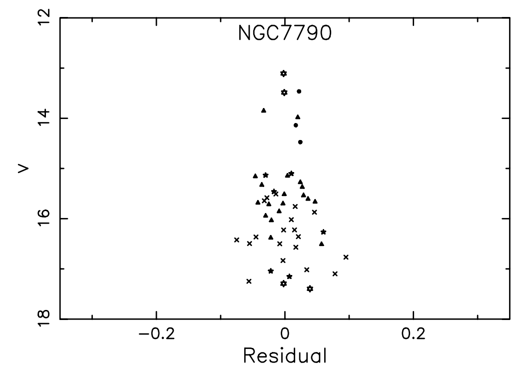

Fig. 4 Relationship between the residuals and v. Here the residual = $(0.15 - 0.002 \times 15.0 - 0.17 \times (b - v)) - (v' - v)$.

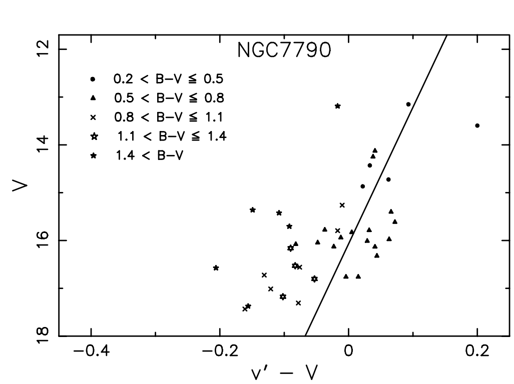

Fig. 5 Relationship between $v' - V$ and V. The straight line represents the equation $v' - V = a_1' + b_1' \times V + c_1' \times (B - V)$ for $(B - V) = 0.65$. Here $b_1' = -0.035$.

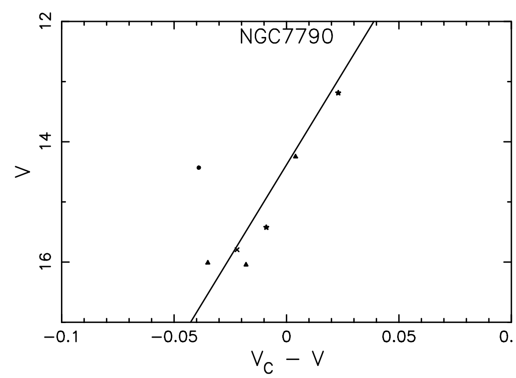

Fig. 6 Relationship between $V_C - V$ and V. Here V_C refers to the photometry of C85. The straight line represents the equation $V_C - V = a_1'' + b_1'' \times V + c_1'' \times (B - V)$ for $(B - V) = 0.65$. Here $b_1'' = -0.016 \pm 0.003$.

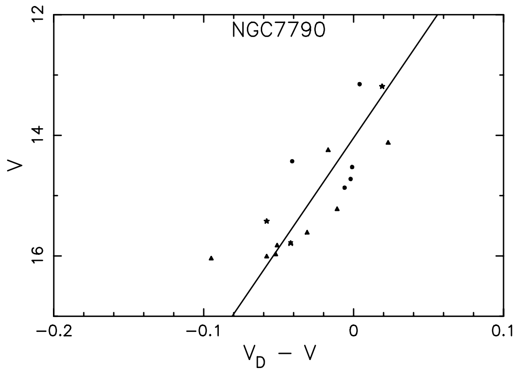

Fig. 7 Relationship between $V_D - V$ and V. Here V_D refers to the photometry of Da99. The straight line represents the equation $V_D - V = a_2 + b_2 \times V + c_2 \times (B - V)$ for $(B - V) = 0.65$. Here $a_2 = 0.39 \pm 0.08$, $b_2 = -0.027 \pm 0.005$, and $c_2 = -0.01 \pm 0.01$.

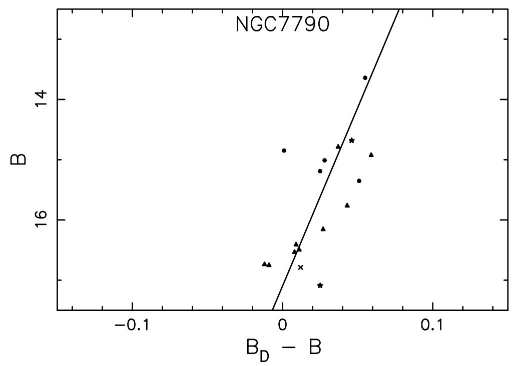

Fig. 8 Relationship between $B_D - B$ and B. Here B_D refers to Da99. The straight line represents the equation $B_D - B = a_3 + b_3 \times B + c_3 \times (B - V)$ for $(B - V) = 0.60$. Here $a_3 = 0.28 \pm 0.06$, $b_3 = -0.017 \pm 0.004$, and $c_3 = -0.02 \pm 0.01$.

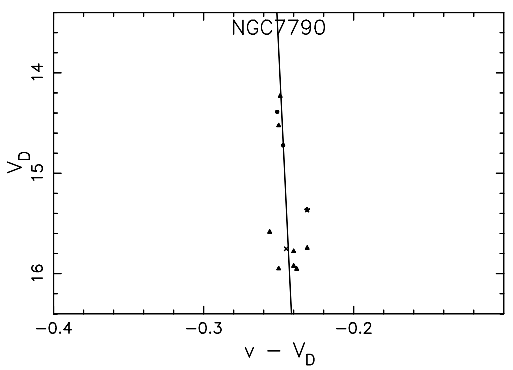

Fig. 9 Relationship between $v - V_D$ and V_D. The straight line represents the equation $v - V_D = a_4 + b_4 \times V_D + c_4 \times (B - V)_D$ for $(B - V)_D = 0.65$. Here $a_4 = -0.30 \pm 0.05$, $b_4 = 0.003 \pm 0.003$, and $c_4 = 0.012 \pm 0.006$.

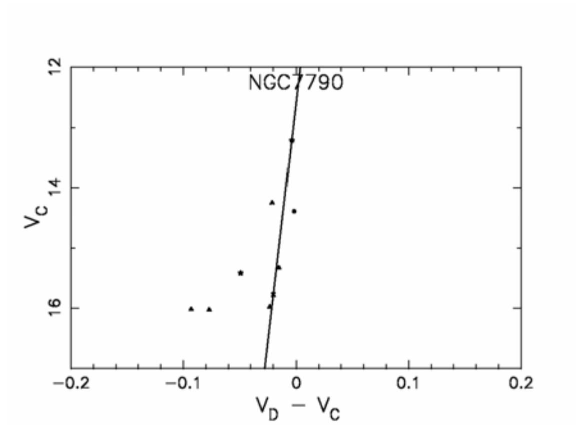

Fig. 10 Relationship between $V_D - V_C$ and V_C. The straight line represents the equation $V_D - V_C = a_5 + b_5 \times V_C + c_5 \times (B - V)_C$ for $(B - V)_C = 0.65$. Here $b_5 = -0.006 \pm 0.004$.

statistics. The comparison is shown in Figure 12 and the scale error so obtained is $b_7 = 0.004 \pm 0.005$, $c_7 = -0.020 \pm 0.009$, and $a_7 = -0.31 \pm 0.08$. At any rate, the scale error is small, if it even exists, in Da99 and C85. Because Stetson (2000) has published his homogeneous photometric standards (Da99's results are transformed into his) the comparison between St00 and Od92 can be made. The comparison of the 44 common stars for V is shown in Figure 13 with $b_8 = -0.040 \pm 0.007$, $c_8 = 0.01 \pm 0.03$, and $a_8 = 0.60 \pm 0.10$; and for B in Figure 14 with $b_9 = -0.027 \pm 0.006$, $c_9 = -0.03 \pm 0.03$, and $a_9 = 0.45 \pm 0.09$. (Od18 is deleted in the calculation for B). The comparison for the R bandpass is shown in Figure 15 with $b_{10} = -0.036 \pm 0.006$, $c_{10} = -0.002 \pm 0.04$, and $a_{10} = 0.51 \pm 0.09$ (star Od76 was deleted in the calculation).

Petrov et al. (2001) did not realize the scale error in Od92. In fact, their declaration of no systematic difference between Od92 and Pe01 means that the scale errors also exist in Pe01. Comparisons between St00 and Pe01 are given in Figures 16, 17, and 18. Here, $b_{11} = -0.018 \pm 0.004$, $c_{11} = -0.05 \pm 0.02$, and $a_{11} = 0.29 \pm 0.06$ for V, $b_{12} = -0.017 \pm 0.004$, $c_{12} = -0.03 \pm 0.02$, and $a_{12} = 0.29 \pm 0.06$ for

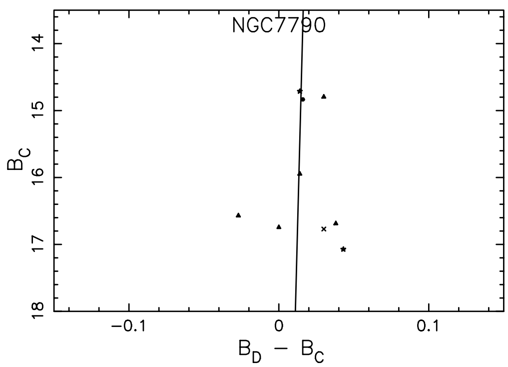

Fig. 11 Relationship between $B_D - B_C$ and B_C. The straight line represents the equation $B_D - B_C = a_6 + b_6 \times B_C + c_6 \times (B - V)_C$ for $(B - V)_C = 0.65$. Here $b_6 = -0.001 \pm 0.008$.

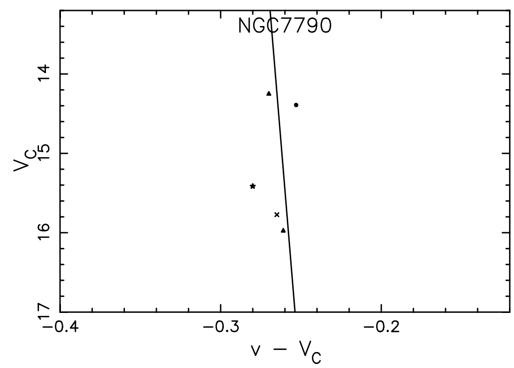

Fig. 12 Relationship between $v - V_C$ and V_C. The straight line represents the equation $v - V_C = a_7 + b_7 \times V_C + c_7 \times (B - V)_C$ for $(B - V)_C = 0.65$. Here $b_7 = 0.004 \pm 0.005$.

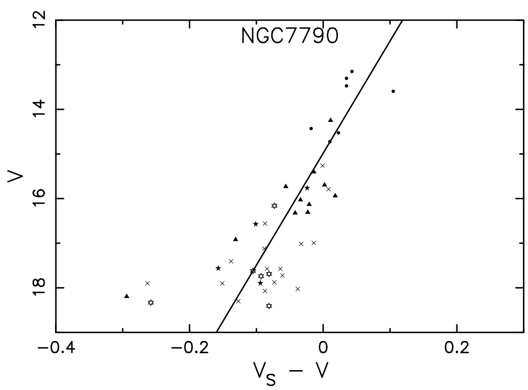

Fig. 13 Relationship between $V_S - V$ and V. The straight line represents the equation $V_S - V = a_8 + b_8 \times V + c_8 \times (B - V)$ for $(B - V) = 0.55$. Here $b_8 = -0.040 \pm 0.007$.

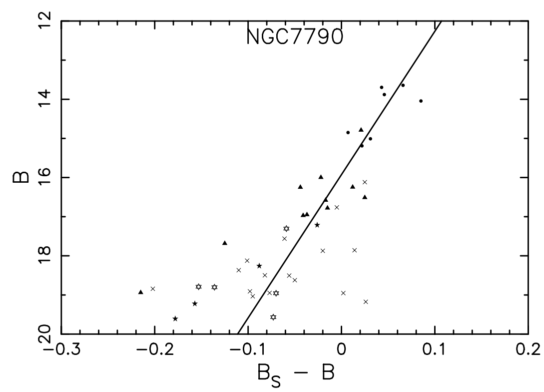

Fig. 14 Relationship between $B_S - B$ and B. The straight line represents the equation $B_S - B = a_9 + b_9 \times B + c_9 \times (B - V)$ for $(B - V) = 0.55$. Here $b_9 = -0.027 \pm 0.006$.

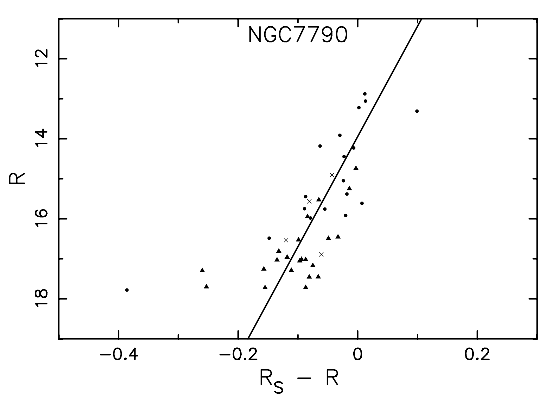

Fig. 15 Relationship between $R_S - R$ and R. The straight line represents the equation $R_S - R = a_{10} + b_{10} \times R + c_{10} \times (V - R)$ for $(V - R) = 0.5$. Here $b_{10} = -0.036 \pm 0.006$.

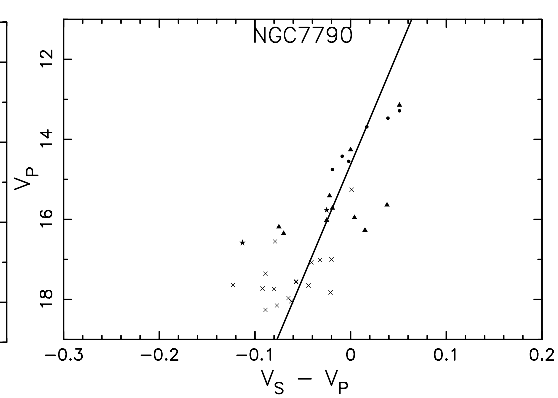

Fig. 16 Relationship between $V_S - V_P$ and V_P. The straight line represents the equation $V_S - V_P = a_{11} + b_{11} \times V_P + c_{11} \times (B - V)_P$ for $(B - V)_P = 0.65$. Here $b_{11} = -0.018 \pm 0.004$.

B, $b_{13} = -0.013 \pm 0.005$, $c_{13} = 0.09 \pm 0.04$, and $a_{13} = 0.19 \pm 0.06$ for R. In addition, the I band photometry of (Pe01) also suffers from the scale error. The comparison between Da99 and Pe01 is in Figure 19 with $b_{14} = -0.04 \pm 0.03$, $c_{14} = 0.12 \pm 0.22$, and $a_{14} = 0.45 \pm 0.38$, and the comparison between St00 and Pe01 in Figure 20 with $b_{15} = -0.036 \pm 0.007$, $c_{15} = 0.08 \pm 0.05$, and $a_{15} = 0.47 \pm 0.09$. As for the U band photometry, comparison between Da99 and Pe01 for 14 common stars shows a rather large scatter, so no definite conclusion can be made (Fig. 21). Here $b_{16} = 0.01 \pm 0.03$, $c_{16} = 0.11 \pm 0.19$, and $a_{16} = -0.22 \pm 0.49$.

We note that there are terms $a_{1U}U_{\rm in}$ and $a_{1I}I_{\rm in}$ in the transformation relations (1) and (2) in Pe01. These terms ($a_{1I} \neq 1$) were only used in photographic photometry in the past. Generally speaking, the coefficients of these terms should always be equal to 1.0 for a linear detector such as a photomultiplier or CCD. We are afraid that it is one of the main causes for their scale error. It is true that the INT data we used show scale errors in the psf analysis. As shown in Figure 22 (96 common stars), the scale error here is $b_{17} = -0.008 \pm 0.002$, $a_{17} = -0.07 \pm 0.04$, and $c_{17} = 0.029 \pm 0.009$. After being transformed to Stetson's system using all the above three coefficients, the resulting magnitudes show no systematic error (Fig. 23). We wish that the INT data we used belong to the special case which does not happen in other instruments. Even for the INT data, it is preferred to use the aperture photometry for isolated stars because the value of the scale error is a function of V itself. It becomes larger when going to fainter stars, and the scatter in Figure 22 is larger than expected. For example, among the 96 common stars, there are 64 isolated or with only faint neighbor stars, so doing aperture photometry with an aperture of $r = 4$ pixels has already almost eliminated the scale error (but a much larger radius must be used for NGC 188 to get the same effect). The obtained magnitudes are transformed into Stetson's system using the common formula $V_S = v + a + c \times (B - V) + d \times (B - V)^2$ (Fig. 24) with less scatter than that in Figure 23.

We have never attempted to let our photometry be standard. As mentioned above, to calibrate our photometry with the standards of Od92 was our purpose, not the reverse. Now, people may use St00 to calibrate their results. If anyone is interested in getting our photometry for the purpose of checking, we can share our results on request.

3 SCALE ERRORS IN THE PHOTOMETRY OF NGC 4147

Unfortunately, the scale errors also exist in the photometry of NGC 4147. The comparisons between the photometry of Od92 and the data taken with the 1.56-m reflector through the V and R filters on 1997 April 6 are given in this paper. Our exposure was 100s for V and 300s for R. As shown in Figures 25 and 26, the random scatter is not small, especially in R (Fig. 26) due to our use of a dome flat-fielding, but it is more than enough to confirm the existence of the scale error. Fitting the relations in Figures 25 and 26 with the equations $v' - V = a_{18} + b_{18} \times V + c_{18} \times (B - V)$ and $r' - R = a_{19} + b_{19} \times R + c_{19} \times (V - R)$ returns the values $a_{18} = 0.84 \pm 0.39$, $b_{18} = -0.05 \pm 0.02$, $c_{18} = -0.02 \pm 0.03$ and $a_{19} = 0.55 \pm 0.23$, $b_{19} = -0.04 \pm 0.01$, $c_{19} = 0.18 \pm 0.05$ (only stars with $0.5 < B - V \leq 0.8$ are used to fit the relation in Fig. 25). Here, v' and r' refer to our instrumental magnitudes and V and R to Od92 as above.

The comparison between Da99 and Od92 is shown in Figure 27. Using the equation $V_D - V = a_{20} + b_{20} \times V + c_{20} \times (B - V)$ to fit the average relation in Figure 27, $a_{20} = 0.45 \pm 0.13$, $b_{20} = -0.025 \pm 0.007$, and $c_{20} = -0.01 \pm 0.02$. Comparison between Da99 and that of the 1.56-m reflector (for V) is given in Figure 28. Here $a_{21} = 0.10 \pm 0.25$, $b_{21} = -0.004 \pm 0.01$, and $c_{21} = -0.03 \pm 0.04$. Though the scatter is large in Figure 27 and not small in Figure 26, the scale error in Figure 25 is definite and mainly comes from Od92.

There are only six common stars between Da99 and C85. As shown in Figure 29 the scatter is large. When the star Od15 (the upper right star in Fig. 29) is deleted in the calculation due to large deviation, no definite conclusion can be obtained for the small number statistics. The least squares solutions for the five common stars are: $a_{22} = -0.09 \pm 0.67$, $b_{22} = 0.006 \pm 0.04$, and $c_{22} = -0.007 \pm 0.06$. However, the scale error appears in the comparison between Od92 and C85, although there are still only six common stars and the star Od15 (the upper left star in Fig. 30) is deleted in the calculation. A similar calculation gives $a_{23} = 0.94 \pm 0.37$, $b_{23} = -0.05 \pm 0.02$, and $c_{23} = -0.07 \pm 0.04$.

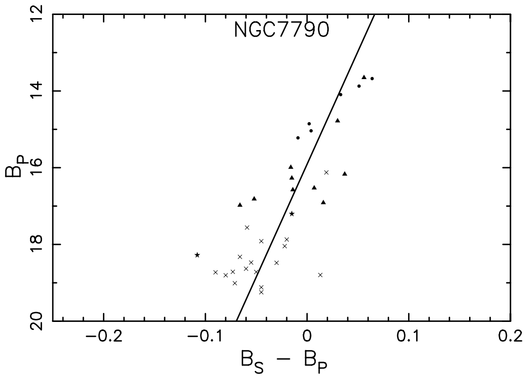

Fig. 17 Relationship between $B_S - B_P$ and B_P. The straight line represents the equation $B_S - B_P = a_{12} + b_{12} \times B_P + c_{12} \times (B-V)_P$ for $(B-V)_P = 0.65$. Here $b_{12} = -0.017 \pm 0.004$.

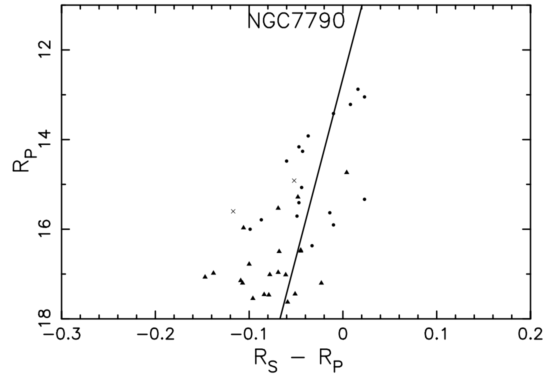

Fig. 18 Relationship between $R_S - R_P$ and R_P. The straight line represents the equation $R_S - R_P = a_{13} + b_{13} \times R_P + c_{13} \times (V-R)_P$ for $(V-R)_P = 0.3$. Here $b_{13} = -0.013 \pm 0.005$.

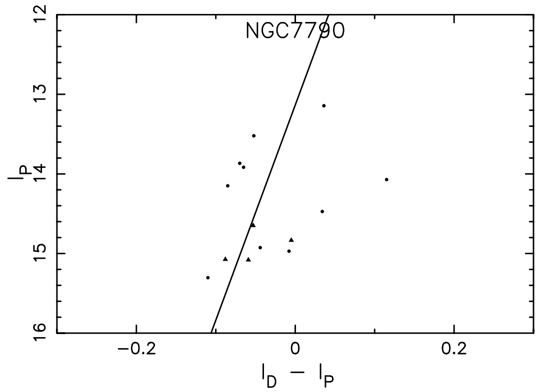

Fig. 19 Relationship between $I_D - I_P$ and I_P. The straight line represents the equation $I_D - I_P = a_{14} + b_{14} \times I_P + c_{14} \times (R-I)_P$ for $(R-I)_P = 0.3$. Here $b_{14} = -0.04 \pm 0.03$.

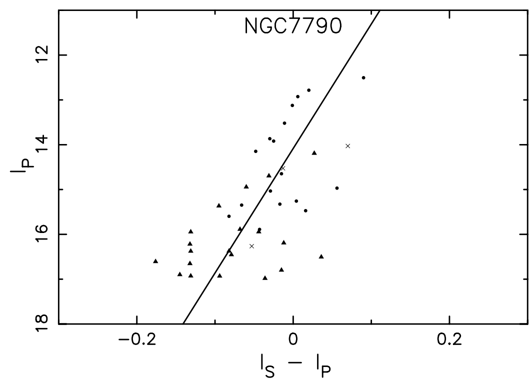

Fig. 20 Relationship between $I_S - I_P$ and I_P. The straight line represents the equation $I_S - I_P = a_{15} + b_{15} \times I_P + c_{15} \times (R-I)_P$ for $(R-I)_P = 0.45$. Here $b_{15} = -0.036 \pm 0.007$.

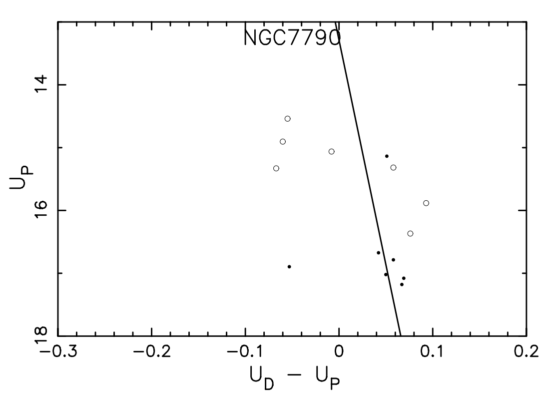

Fig. 21 Relationship between $U_D - U_P$ and U_P. The straight line represents the equation $U_D - U_P = a_{16} + b_{16} \times U_P + c_{16} \times (R-I)_P$ for $(U-B)_P = 0.3$. Here $b_{16} = 0.01 \pm 0.03$.

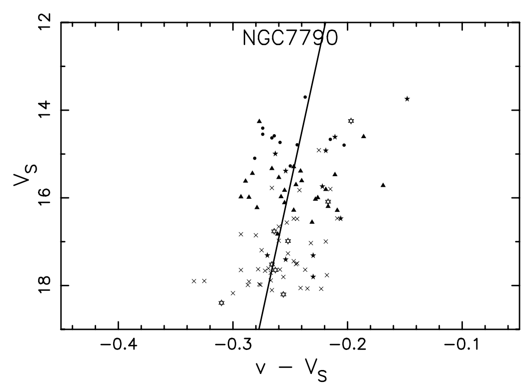

Fig. 22 Relationship between $v - V_S$ and V_S. The straight line represents the equation $v - V_S = a_{17} + b_{17} \times V_S + c_{17} \times (B-V)_S$ for $(B-V)_S = 0.6$. Here $b_{17} = -0.008 \pm 0.002$.

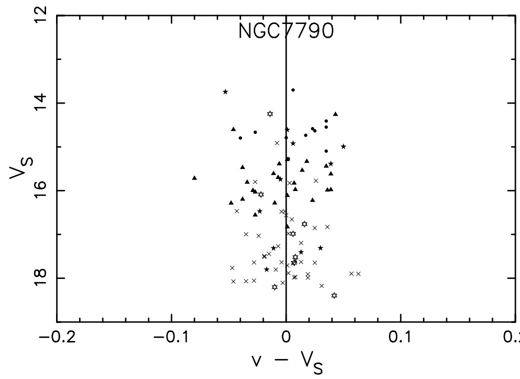

Fig. 23 Relationship between $v - V_S$ and V_S. Here, our v magnitudes have been transformed into V_S. The straight line shows no systematic error.

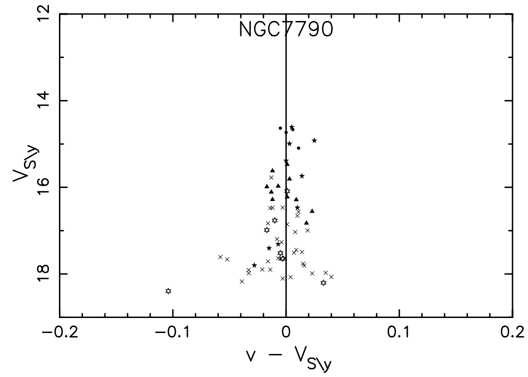

Fig. 24 Relationship between $v - V_S$ and V_S. Here, our v magnitudes are obtained from aperture photometry and transformed into V_S without using the scale term. The straight line shows no systematic error.

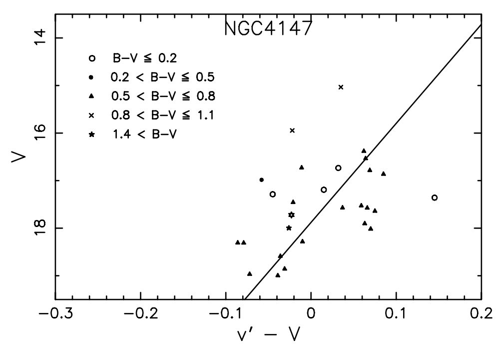

Fig. 25 Relationship between $v' - V$ and V. The straight line represents the equation $v' - V = a_{18} + b_{18} \times V + c_{18} \times (B - V)$ for $(B - V) = 0.65$. Here $b_{18} = -0.05 \pm 0.02$.

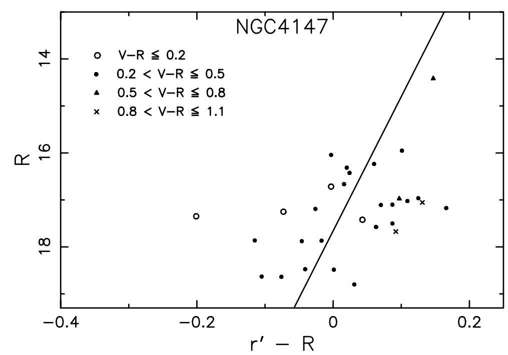

Fig. 26 Relationship between $r' - R$ and R. The straight line represents the equation $r' - R = a_{19} + b_{19} \times R + c_{19} \times (V - R)$ for $(V - R) = 0.35$. Here $b_1 = -0.04 \pm 0.01$.

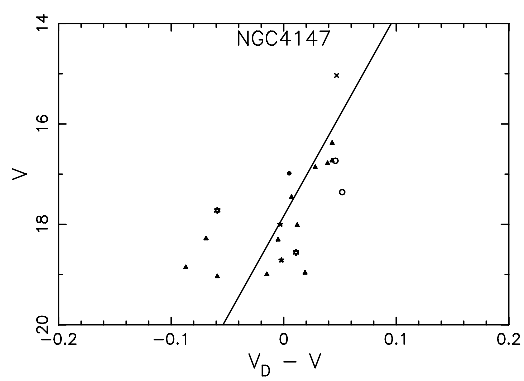

Fig. 27 Relationship between $V_D - V$ and V. The straight line represents the equation $V_D - V = a_{20} + b_{20} \times V + c_{20} \times (B - V)$ for $(B - V) = 0.65$. Here $b_{20} = -0.025 \pm 0.007$.

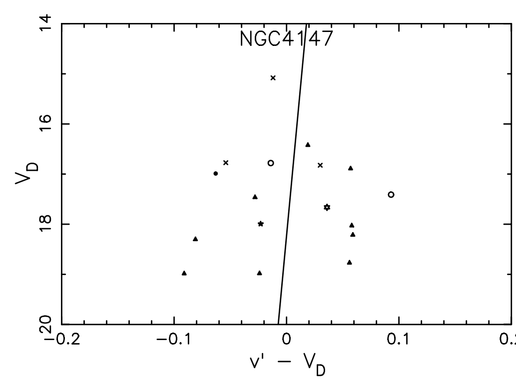

Fig. 28 Relationship between $v' - V_D$ and V_D. The straight line represents the equation $v' - V_D = a_{21} + b_{21} \times V_D + c_{21} \times (B - V)_D$ for $(B - V)_D = 0.65$. Here $b_{21} = -0.004 \pm 0.01$.

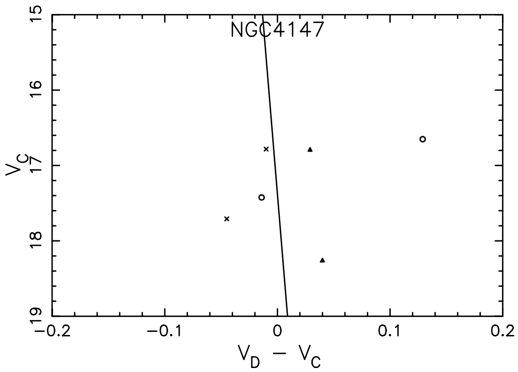

Fig. 29 Relationship between $V_D - V_C$ and V_C. The straight line represents the equation $V_D - V_C = a_{22} + b_{22} \times V_C + c_{22} \times (B - V)_C$ for $(B - V)_C = 0.65$. Here $b_{22} = 0.006 \pm 0.04$.

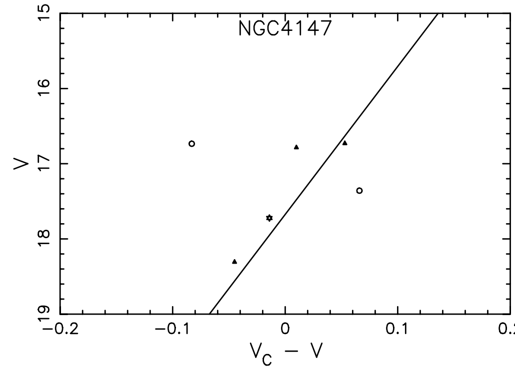

Fig. 30 Relationship between $V_C - V$ and V. The straight line represents the equation $V_C - V = a_{23} + b_{23} \times V + c_{23} \times (B - V)$ for $(B - V) = 0.65$. Here $b_{23} = -0.05 \pm 0.02$.

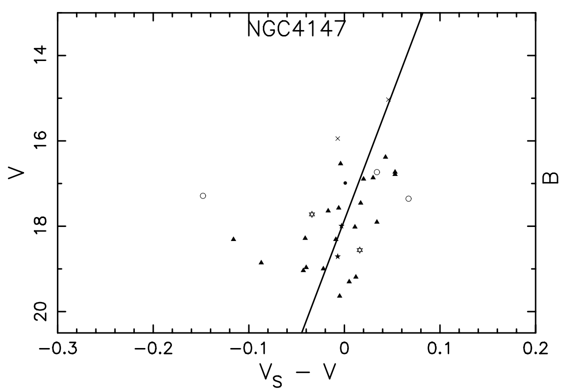

Fig. 31 Relationship between $V_S - V$ and V. The straight line represents the equation $V_S - V = a_{24} + b_{24} \times V + c_{24} \times (B - V)$ for $(B - V) = 0.95$. Here $b_{24} = -0.017 \pm 0.007$.

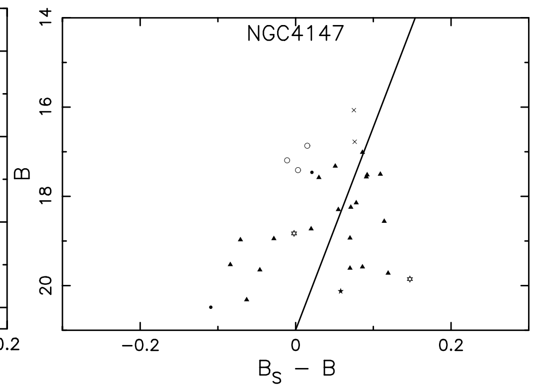

Fig. 32 Relationship between $B_S - B$ and B. The straight line represents the equation $B_S - B = a_{25} + b_{25} \times B + c_{25} \times (B - V)$ for $(B - V) = 0.9$. Here $b_{25} = -0.022 \pm 0.009$.

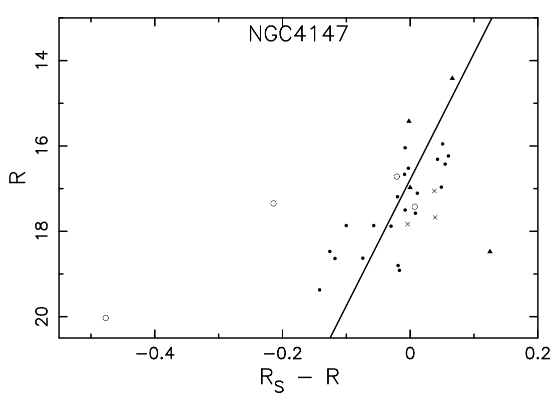

Fig. 33 Relationship between $R_R - R$ and R. The straight line represents the equation $R_S - R = a_{26} + b_{26} \times R + c_{26} \times (V - R)$ for $(V - R) = 0.4$. Here $b_{26} = -0.034 \pm 0.007$.

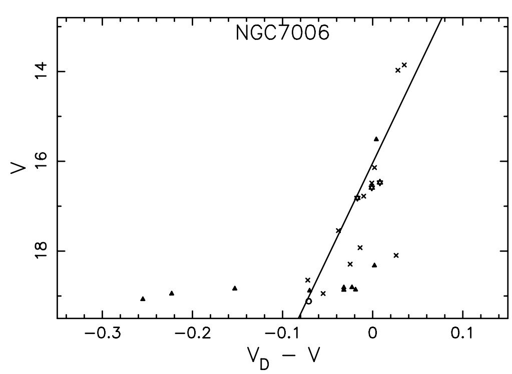

Fig. 34 Relationship between $V_D - V$ and V. The straight line represents the equation $V_D - V = a_{27} + b_{27} \times V + c_{27} \times (B - V)$ for $(B - V) = 0.9$. Here $b_{27} = -0.024 \pm 0.009$.

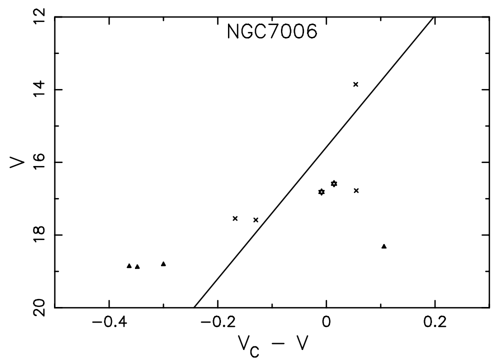

Fig. 35 Relationship between $V_C - V$ and V. The straight line represents the equation $V_C - V = a_{28} + b_{28} \times V + c_{28} \times (B-V)$ for $(B-V) = 0.9$. Here $b_{28} = -0.06 \pm 0.03$.

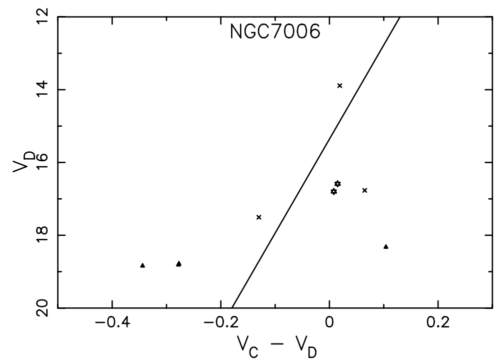

Fig. 36 Relationship between $V_C - V_D$ and V_D. The straight line represents the equation $V_C - V_D = a_{29} + b_{29} \times V_D + c_{29} \times (B-V)_D$ for $V_D = 0.9$. Here $b_{29} = -0.04 \pm 0.04$.

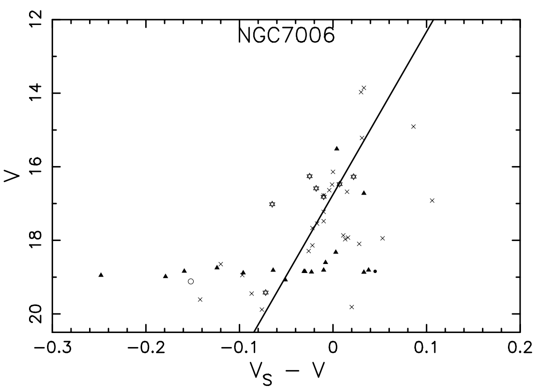

Fig. 37 Relationship between $V_S - V$ and V. The straight line represents the equation $V_S - V = a_{30} + b_{30} \times V + c_{30} \times (B-V)$ for $(B-V) = 0.6$. Here $b_{30} = -0.023 \pm 0.006$.

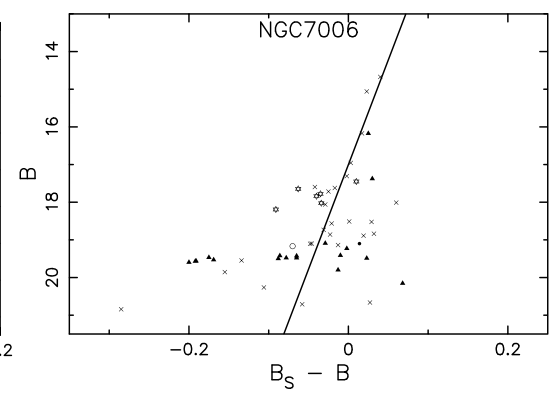

Fig. 38 Relationship between $B_S - B$ and B. The straight line represents the equation $B_S - B = a_{31} + b_{31} \times V + c_{31} \times (B-V)$ for $(B-V) = 1.0$. Here $b_{31} = -0.018 \pm 0.008$.

The comparisons between Od92 and St00 are shown in Figures 31, 32, and 33. Here, $b_{24} = -0.017 \pm 0.007$, $a_{24} = 0.28 \pm 0.13$, and $c_{24} = 0.03 \pm 0.03$ for V (Od111, 128 deleted in calculation), $b_{25} = -0.022 \pm 0.009$, $a_{25} = 0.38 \pm 0.17$, and $c_{25} = 0.09 \pm 0.04$ for B (here the scatter is large), $b_{26} = -0.034 \pm 0.007$, $a_{26} = 0.54 \pm 0.12$, and $c_{26} = 0.06 \pm 0.03$ for R (Od111, 135, 103 are deleted in calculation).

3.1 Scale Errors in the Photometry of NGC 7006

Now that scale errors exist in the photometry of NGC 7790 and NGC 4147, it is expected that the scale error exists in the photometry of NGC 7006 because the same CCD system and technique were used to measure the three standard fields. That is indeed the case. Here, we compare Da99 and Od92 (Fig. 34). In Figure 34, the two bright stars near $V = 14$ are omitted in Da99 but are included in the list given to Odewahn et al. (1992). These two stars plotted in the figure show the varied scale error more clearly. Fitting the relation with the equation $V_D - V = a_{27} + b_{27} \times V + c_{27} \times (B-V)$, $b_{27} = -0.024 \pm 0.009$, $a_{27} = 0.35 \pm 0.18$, and $c_{27} = 0.04 \pm 0.05$. Notice for the stars fainter than $V = 18.5$ (where the photometry becomes less reliable, Davis 1999), it seems that there is a large scale error for the faintest stars. Comparing Od92 with C85, the large scale error begins at about $V = 16.5$ (Fig. 35). The solutions for the equation fitting the relation in Figure 35 are: $a_{28} = 0.60 \pm 0.69$, $b_{28} = -0.06 \pm 0.03$, and $c_{28} = 0.29 \pm 0.21$. It was pointed out (Yao 1998) that in the photographic photometry for NGC 7006 there is a large scale error which begins at about $V = 18.5$ that was obtained by comparing with Od92. Now the conclusion should be modified because during that time, the scale error in Od92 was not recognized. The scale error shown in that paper (Yao 1998) at least partly came from Od92 themselves. The comparison between C85 and Da99 is shown in Figure 36. It is true that the photoelectric photometry of C85 is not accurate in NGC 7006 for the faint stars. However, the reason that the three faintest stars (near $V = 19$) also show large scale errors (similar to that in Fig. 35) is not easily understood. Can the error from C85 be partly due to the difficulty with the sky measurements (including the unseen faint stars in the diaphragm of the photometer)? We do not know. To fit the relation in Figure 36 with a linear equation may be less meaningful, here, $a_{29} = 0.34 \pm 0.71$, $b_{29} = -0.04 \pm 0.04$, and $c_{29} = 0.29 \pm 0.20$.

The comparisons between St00 and Od92 are given in Figures 37 and 38. The large scale errors for faint ($V > 18.5$ in Fig. 37 and $B > 19$ in Fig. 38) stars are still obvious. Here $b_{30} = -0.023 \pm 0.006$, $a_{30} = 0.38 \pm 0.11$, and $c_{30} = 0.003 \pm 0.03$ for V (Od41 deleted in calculation), $b_{31} = -0.018 \pm 0.008$, $a_{31} = 0.28 \pm 0.16$, and $c_{31} = 0.03 \pm 0.04$ for B (Od185, 198 are deleted in calculation).

To make the comparisons among different observations more compact and clear, the results are combined into Table 1.

Table 1 Transformation Coefficients among Different Observations

System 1	System 2	Zero point	Scale	Color term	Note
Od92 (V)	YC[a] (v)	0.29±0.08	–0.036±0.005	0.01±0.02	Fig. 1
Od92 (B)	YC (b)	0.40±0.05	–0.031±0.003	–0.08±0.01	Fig. 2
YC (v)	1.56-m (v)	0.15±0.08	–0.002±0.005	–0.17±0.02	Fig. 3
Od92 (V)	1.56-m (v)	0.65±0.10	–0.035±0.007	–0.13±0.02	Fig. 5
Od92 (V)	C85 (V)	0.23±0.05	–0.016±0.003	0.005±0.008	Fig. 6
Od92 (V)	Da99 (V)	0.39±0.08	0.027±0.005	–0.01±0.01	Fig. 7
Od92 (B)	Da99 (B)	0.28±0.06	–0.017±0.004	–0.02±0.01	Fig. 8
Da99 (V)	YC (v)	–0.30±0.05	0.003±0.003	–0.012±0.006	Fig. 9
C85 (V)	Da99 (V)	0.08±0.06	–0.006±0.004	–0.001±0.001	Fig. 10
C85 (B)	Da99 (B)		–0.001±0.008		Fig. 11
C85 (V)	YC (v)	–0.31±0.08	0.004±0.005	–0.020±0.009	Fig. 12
Od92 (V)	St00 (V)	0.60±0.10	–0.040±0.007	0.01±0.03	Fig. 13
Od92 (B)	St00 (B)	0.45±0.09	–0.027±0.006	0.03±0.03	Fig. 14
Od92 (R)	St00 (R)	0.51±0.09	–0.036±0.006	–0.002±0.04	Fig. 15
Pe01 (V)	St00 (V)	0.29±0.06	–0.018±0.004	–0.05±0.02	Fig. 16
Pe01 (B)	St00 (B)	0.29±0.06	–0.017±0.004	–0.03±0.02	Fig. 17
Pe01 (R)	St00 (R)	0.19±0.06	–0.013±0.005	0.09±0.04	Fig. 18
Pe01 (I)	Da99 (I)	0.45±0.38	–0.04±0.03	0.12±0.22	Fig. 19
Pe01 (I)	St00 (I)	0.47±0.09	–0.036±0.007	0.08±0.05	Fig. 20
Pe01 (U)	Da99 (U)	–0.22±0.49	0.01±0.03	0.11±0.19	Fig. 21
St01 (V)	YC (v)	–0.07±0.04	–0.008±0.002	0.029±0.009	Fig. 22 (psf)
St01 (V)	YC (v)	0.22±0.03	0.0±0.0	–0.09±0.06	Fig. 24 (aper.)[b]
Od92 (V)	1.56-m (v)	0.84±0.39	–0.05±0.02	–0.02±0.03	Fig. 25
Od92 (R)	1.56-m (r)	0.55±0.23	–0.04±0.01	0.18±0.05	Fig. 26
Od92 (V)	Da99 (V)	0.45±0.13	–0.025±0.007	–0.01±0.02	Fig. 27
DA99 (V)	YC (V)	0.10±0.25	–0.004±0.01	–0.03±0.04	Fig. 28
C85 (V)	Da99 (V)	–0.09±0.67	0.006±0.04	–0.007±0.06	Fig. 29
Od92 (V)	C85 (V)	0.94±0.37	–0.05±0.02	–0.07±0.04	Fig. 30
Od92 (V)	St00 (V)	0.28±0.13	–0.017±0.007	0.03±0.03	Fig. 31
Od92 (B)	St00 (B)	0.38±0.17	–0.022±0.009	0.09±0.04	Fig. 32
Od92 (R)	St00 (R)	–0.54±0.12	–0.034±0.007	0.06±0.03	Fig. 33
Od92 (V)	Da99 (V)	0.35±0.18	–0.024±0.009	0.04±0.05	Fig. 34
Od92 (V)	C85 (V)	0.60±0.69	–0.06±0.03	0.29±0.21	Fig. 35
Da99 (V)	C85 (V)	0.34±0.71	–0.04±0.04	0.29±0.20	Fig. 36
Od92 (V)	St00 (V)	0.38±0.11	–0.023±0.006	0.003±0.03	Fig. 37
Od92 (B)	St00 (B)	0.28±0.16	–0.018±0.008	0.03±0.04	Fig. 38

Notes: a. YC refers to the instrumental magnitudes of INT reduced by the authors;
b. Here the transformation has another term "$d \times (B - V)^2$", $d = 0.03 \pm 0.03$.

4 DISCUSSION

The reason why the scale errors, which may only appear in photographic photometry, exist in a linear detector like CCD is not clear. As far as we know, in the past we were always told that the CCD has both the advantages of photoelectric and photographic photometry, such as being highly linear, etc. Almost all CCD systems were checked for linearity before being attached to the telescope, especially for those observatories where it is not easy to get a scientific grade CCD system. Later, it was heard that some CCD systems may be nonlinear if the electric part was not correctly made and adjusted. The first case reported in astronomical literature may be the Tek 2048 system non-linearity at the 1.5-m of CTIO found by P. Stetson (Walker 1993), at the level of almost 2 percent per magnitude. After the CCD FET bias voltages were re-optimized, that Tek 2048 becomes linear to about 0.1 percent. If the RCA CCD used by Odewahn et al. (1992) did not suffer from this kind of trouble, maybe it is related to their use of the variable aperture technique. If this were the case, the original data of Od92 might be reduced again using the point spread function analysis technique such as that in DAOPHOT without re-observing.

The photometry of Da99 was also made with an RCA 320×512 CCD. The aperture photometry was used through a smallish aperture to maximize the signal-to-noise ratio and then the aperture correction was applied. For isolated stars, the aperture photometry is the best. However, to isolate the real isolated stars, it is better to first use a large telescope with a long focal length. While it is certain that the photometry of Da99 has no large scale errors, for the time being, it is not absolutely definite that it does not suffer from small scale errors.

When the demand to combine existing photometry into an integrated table is raised, we do not think it is suitable to correct the scale errors in Od92 by others. In a transformation equation $V - v = v + a + b \times v + c \times (b - v)$, if b is not zero but forced to be zero, the solutions for a and c will be systematically wrong, especially in a cluster where the magnitude has a dependence on the color. So, the published results mix the scale error and color equation. The value of b itself varies from bright to faint stars, so it is difficult to correct. The best way is to correct the scale error in the raw data first, instead of correcting it later.

Acknowledgements This work was supported by the United Laboratory of Optical Astronomy, CAS and a grant from the “Climb Project”. Thanks to Drs. Griffiths and Buttress for getting the data at INT. Permission to use her unpublished photometry by Dr. L. Davis is gratefully acknowledged. We also thank Dr. P. Stetson for helpful suggestions.

References

Christian, C. A., Adams, M., Barnes, J. V., Butcher, H., Hayes, D. S., Mould, J. R., & Siegel, M. 1985, PASP, 97, 363 (C85)
Davis, L. 1999, private communication
Massey, P. & Davis, L. E. 1992, A User’s Guide to Stellar CCD Photometry with IRAF
Odewahn, S. C., Bryja, C., & Humphreys, R. M. 1992, PASP, 104, 553 (Od92)
Petrov, G., Seggewiss, W., Dieball, A., & Kovachev, B. 2001, A&A, 376, 745 (Pe01)
Stetson, P. B. 1987, PASP, 99, 191
Stetson, P. B. 2000, PASP, 112, 925 (St00)
Unger, S. W., Brinks, E., Laing, R. A., Tritton, K. P., & Gray, P. M. 1988, Observers’ Guide (Isaac Newton Group, La Palma 1988)
Walker, A. 1993, NOAO Newsletter, 34, 9
Yao, B. A. 1998, Acta Astron. Sin., 39, 225